Estimation of Shadowing Effects in Millimeter-wave Short Range Communication by Equivalent Edge Current

Maifuz Ali[(1)] and Makoto Ando[(2)]

[(1)] International Institute of Information Technology, Naya Raipur, Chhattisgarh, India
[(2)] Tokyo Institute of Technology, Tokyo, Japan

***Abstract*—The 60 GHz band compact-range communication is very promising for short-time, short distance communication. Unfortunately, due to the short wavelengths in this frequency band the shadowing effects caused by human bodies, furniture, etc are severe and need to be modeled properly. The numerical methods like the finite-difference time-domain method (FDTD), the finite-element method (FEM), the method of moments (MoM) are unable to compute the field scattered by large objects due to their excessive time and memory requirements. Ray-based approaches like the geometrical theory of diffraction (GTD), uniform geometrical theory of diffraction (UTD), uniform asymptotic theory of diffraction (UAT) of diffraction are effective and popular solutions but suffer from computation of corner diffraction, field at the caustics. Fresnel zone number (FZN) adopted modified edge representation (MER) equivalent edge current (EEC) is an accurate and fast high frequency diffraction technique which expresses the fields in terms of line integration. It adopts distances, rather than the angles used in GTD, UTD or UAT but still provides uniform and highly accurate fields everywhere including geometrical boundaries. The dipole wave scattering from flat rectangular plates is discussed with numerical examples.**

I. Introduction

Next generation wireless systems operating in the 60 GHz band are currently being designed to provide very high data rates for short range communications. Authors in [1], [2] have proposed a new concept named compact range communication, where users in the quasi-plane wave illumination zone are almost free of multi-paths. The free-space loss in the millimeter wave band is comparatively large, essential where directional antenna is used. In addition, large propagation loss due to obstacles in the propagation path, like propagation loss generated by the human body, which is not a problem in microwave band is also the matter of concern in millimeter wave band. The human body shadowing effect is a communication disconnection problem in this communication system especially in the dense populated public places. An accurate and simple evaluation of the fields in the shadow region due to the three dimensional scatterers like human bodies is the key issue for evaluating the communication performances of the system.

Full wave solutions by numerical techniques (e.g. finite difference time domain, finite-element, and method of moments) are computationally infeasible due to the small wavelengths of the millimeter band. Geometrical theory of diffraction (GTD) [3] or uniform geometrical theory of diffraction (UTD) [4], uniform asymptomatic theory of diffraction (UAT) [5]–[7] are very efficient ray techniques for high frequencies. But these methods have disadvantages like infinite fields at the caustics, singularities at incidence/reflection shadow boundaries (ISB/RSB) and negligence of corner diffraction.

The method of modified edge representation (MER) equivalent edge currents (EECs) by line integration along the edge of scatterers, capable of eliminating difficulties of caustics and corner diffraction is very efficient and accurate for high frequency diffraction [8]. The classical Keller's diffraction coefficients [3] were used directly with respect to modified edge [8]. For simplicity, trigonometric functions of the Keller's diffraction coefficients are replaced by the path lengths between source and the point of integration, path lengths between the point of integration and the observer and the direct path between the source and the observer [9]. These are reformed into the expression of the Fresnel zone number (FZN) which may be familiar to the wireless system designers. This FZN MER method is reformed so that the communication system designers who are not familiar to the high frequency field analysis may use it easily without specific knowledge of diffraction.

For validation of the method and demonstration of the advantage in terms of computational load and time, the scattering of a dipole wave from a rectangular plate is considered and the results are compared with method of moment-based commercial em-solver Wipl-D [10]. Secondly, two rectangular plates in the geometrically staggered position with geometrical overlapping are considered. Some integration points are not visible geometrically from the source or the observer position. By simply excluding these non-visible parts from MER EEC line integration and without taking any mutual coupling between the plates or multiple diffraction into account, the proposed MER provides reasonable comparison with the results by MoM (Wipl-D). Due to the limitation of the memory requirement of Wipl-D, accuracy comparison is limited at the frequency 10 GHz for the objects with the actual size of human body. Shadowing effects due to the same size of scatterers at 60 GHz frequency are also presented.

II. Equivalent Edge Current and the Diffracted Field [11], [12]

The method enabling the surface to line integral reduction is the key element in deriving the equivalent edge currents

(EECs). A concept of modified edge representation(MER), which extends the definition of EEC for diffraction points to those for general edge points was introduced in [11], [12]. Classical Keller's diffraction coefficients were adopted for the computations of the diffracted field as follows.

For two polarization, soft and hard boundary conditions are applied and the equivalent edge currents (EECs) along the edge of the scatterer $\hat{e}$ are given by [13, eq. (13-103)],

$$\overrightarrow{I_s} = -\frac{\sqrt{8\pi k}}{\eta k} e^{-\jmath\pi/4} E^i_{\beta_i}(Q) D_s \hat{e} \tag{1a}$$

$$\overrightarrow{I_h} = -\frac{\sqrt{8\pi k}}{\eta k} e^{-\jmath\pi/4} E^i_{\phi_i}(Q) D_h \hat{e} \tag{1b}$$

where D_s & D_h are the diffraction coefficients at the point Q for soft and hard boundary conditions respectively and the Keller's diffraction coefficient of [3, eq. (2)] is

$$D^{GTD}_{s,h} = \frac{-e^{\jmath\pi/4}}{2\sqrt{2\pi k}\sin\beta_i}\left[\sec\left(\frac{\phi_o - \phi_i}{2}\right) \mp \sec\left(\frac{\phi_o + \phi_i}{2}\right)\right] \tag{2}$$

The diffraction fields are expressed as the line radiation integrals of the equivalent edge currents along the peripheries of the scatterers, as follows.

$$\overrightarrow{E^d_s} = \frac{\jmath\eta k}{4\pi}\oint \hat{r_o} \times \left[\hat{r_o} \times \overrightarrow{I_s}\right]\frac{e^{-jk|r_o|}}{|r_o|}dl \tag{3a}$$

$$\overrightarrow{E^d_h} = \frac{\jmath\eta k}{4\pi}\oint \left[\hat{r_o} \times \overrightarrow{I_h}\right]\frac{e^{-jk|r_o|}}{|r_o|}dl \tag{3b}$$

III. Numerical results of shadowing effects from Two Scatterers in Staggered Arrangement

A. Case where every edge is visible from both the source and the observer

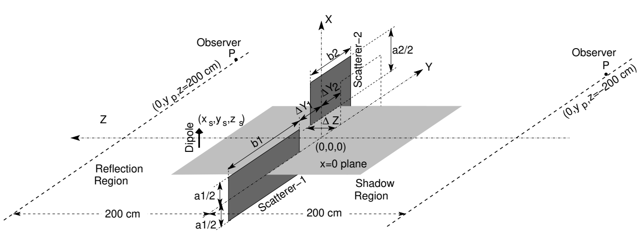

Fig. 1: Schematic diagram of two staggered rectangular plates before a dipole

Two PEC plates with $a_1 = 30$ cm, $b_1 = 60$ cm, $a_2 = 60$ cm, $b_2 = 30$ cm, $\Delta Y_1 = \Delta Y_2 = 30$ cm, $\Delta Z = 30$ cm and a dipole at (0,0,57 cm) are consider as in the Fig. 1. The shadow and reflected regions that are created by the plates and dipole on $x = 0$ plane are shown in Fig. 2.

As, MER belongs to the high frequency approximation, only single edge diffraction, as the lowest order, is considered for this computation. The higher order contributions varies with the mutual arrangement of the two plates and are called as mutual coupling or multiple diffraction etc here. Without taking any mutual coupling between the plates and multiple

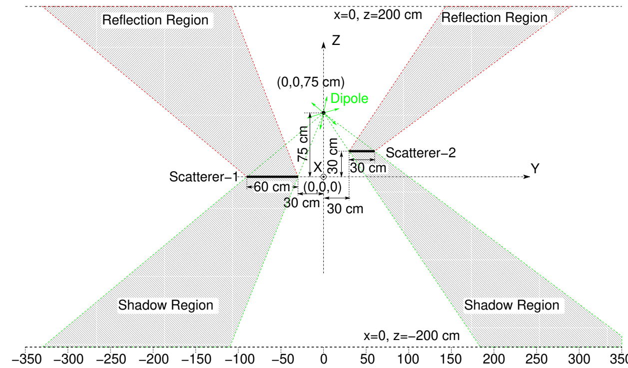

Fig. 2: Top view (x=0 plane) of the scatterer of Fig. 1 with shadow and reflection region.

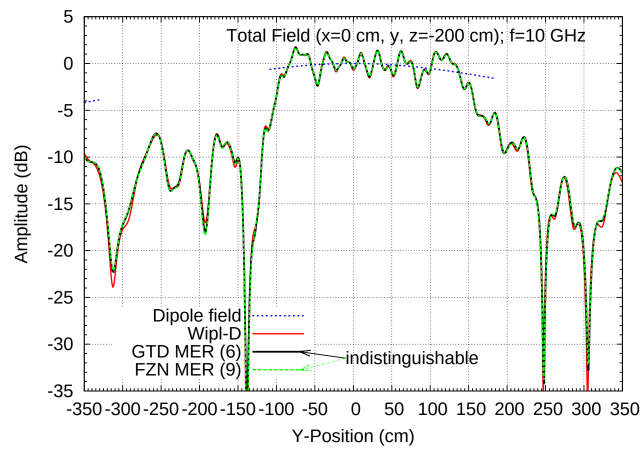

Fig. 3: Filed at 10 GHz in the shadow region, along $x = 0,\ y,\ z = -200$ corresponding to the Fig. 2.

diffraction between edges of the plate, FZN MER and GTD MER computed fields at 10 GHz in the shadow region along $x = 0,\ y,\ z = -200$ cm (in $x = 0$ plane) are compared with Wipl-D simulation results shown in the Fig. 3. The FZN MER and GTD MER computed results are indistinguishable and well matched with the Wipl-D simulated results in full length of observation.

B. Cases where some edges are not visible from the source or the observer

Tow scatterer of Fig. 1 are shifted from $\Delta Y_1 = \Delta Y_2 = 30$ cm to $\Delta Y_1 = \Delta Y_2 = -10$ cm. Now the plates look like overlaped when seen from the source or some position of the observer. The front, side and top views are shown in the Fig. 4. The fields are computed in the shadow region at $z = -200$ cm detailed below.

1) Field along $x = 0,\ y,\ z = -200$ cm: As, we have already shown that the FZN MER result is identical and indistinguishable with GTD MER, in this case only FZN MER result is compared with Wipl-D results for the field at the shadow region along $x = 0,\ y,\ z = -200$ cm shown in the Fig. 5. FZN MER fields are well matched with the Wipl-D simulated field for observation at $y < ISB_1(-180$ cm$)$ and

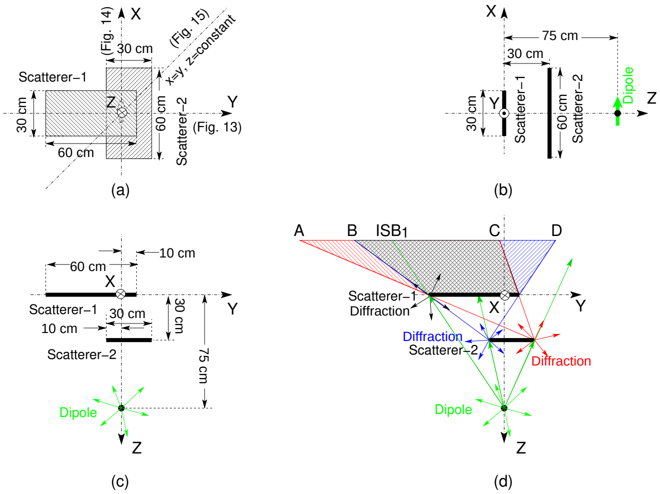

Fig. 4: Stagger with overlap arrangement of two rectangular plates (a) front view (b) side view (c) top view (d) top view of double diffraction.

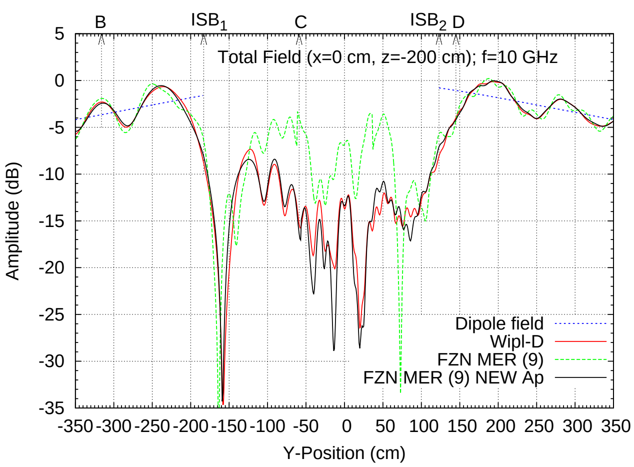

Fig. 5: Field at 10 GHz in the shadow region, along $x = 0,\ y,\ z = -200$ cm corresponding to the Fig. 4

$y > ISB_2$(123 cm). But within the ISBs (from $y = -180$ cm to $y = 123$ cm), a huge difference in FZN MER and Wipl-D field is observed.

From the Fig. 4, it is clear that some integration points along the periphery of the scatterer-1 are not visible from the source due the obstetrical contributed by scatterer-2. Similarly some integration points in the scatterer-2 are not visible from some position of the observer due the obstetrical contributed by scatterer-1. The invisible integration point from the source on scatterer-1 will not contribute the field at the observation and similarly the invisible integration point from the observer on scatterer-2 will not contribute the field at the observation. $x = 0$ planer views of these points are shown in Fig. 4(d). The unseen points of integration of scatterer-1 and scatterer-2 from the source and the observer respectively are excluded from the MER integration. Without taking any mutual coupling between two plates and multiple diffraction between the edged, the results by this new approximation is shown in the Fig. 5 as "FZN MER NEW Ap". Now the agreement with Wipl-D result is very good in almost all point of observations.

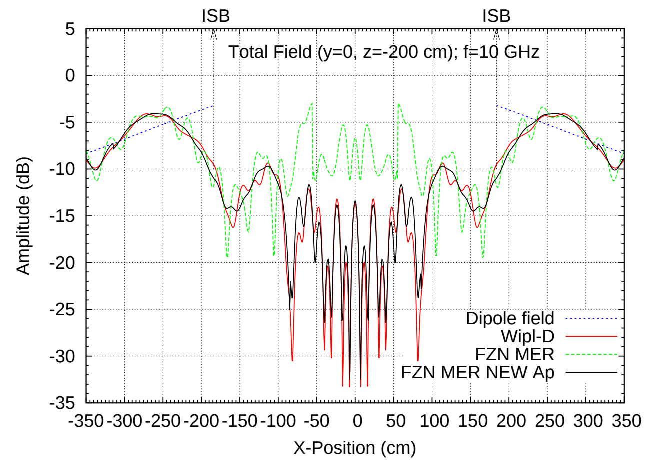

Fig. 6: Field at 10 GHz in the shadow region, along $x,\ y = 0,\ z = -200$ cm corresponding to the Fig. 4

2) Field along $x,\ y = 0,\ z = -200$ cm: Computed field using FZN MER and FZN MER with new approximation (FZN MER NEW Ap) along $x,\ y = 0,\ z = -200$ cm are compared with the Wipl-D result shown in Fig. 6. This figure shows very good agreement of new approximation of FZN MER with Wipl-D simulation.

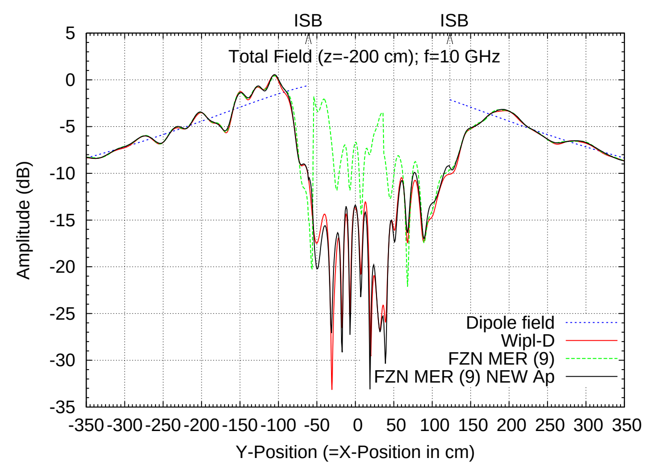

Fig. 7: Field at 10 GHz in the shadow region, along $x = y,\ z = -200$ cm (in diagonal plane) corresponding to the Fig. 4.

3) Field along $x = y,\ z = -200$: In the diagonal plane, along $x = y,\ z = -200$ cm, the field using FZN MER and FZN MER with new approximation (FZN MER NEW Ap) are compared with the Wipl-D result shown in Fig. 7. This result again shows very good agreement of new approximation of FZN MER with the Wipl-D results.

For the computation of field of Figs. 5, 6, and 7, multiple diffraction between the edges in the same plate and the mutual coupling effects between the two plates are not considered. For these reasons, the small ripples in the WiPL-D results are not explained by the result of FZN MER with new approximation (FZN MER (9) New Ap). Note that these effects decrease with the increase of frequency and in the millimeter could be acceptable.

C. Shadowing Effects at 60 GHz

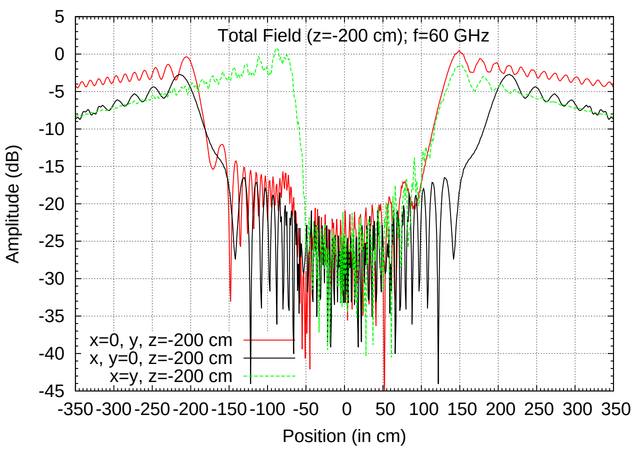

Fig. 8: Field at 60 GHz in the shadow region, along ($x = 0,\ y,\ z = -200$ cm), ($x,\ y = 0,\ z = -200$ cm) and ($x = y,\ z = -200$ cm) corresponding to the Fig. 4.

With the frequency increased 6 times that of Sec. III-B i.e. for frequency 60 GHz, fields along ($x = 0,\ y,\ z = -200$ cm), ($x,\ y = 0,\ z = -200$ cm), and ($x = y,\ z = -200$ cm) due to the scatterer of the same size of the Fig. 4, are shown in the Fig. 8, without reference solution due to the memory size limitation of Wipl-D.

However, from Figs. 5, 6, 7, and 8 it is conclude that at 60 GHz, radio channel is more sensitive to shadowing in compared to 10 GHz due to high attenuation of non-line-of-sight (NLOS) propagation.

IV. Conclusion

Modified edge representation (MER) is demonstrated for compact rang communication. First, the method is verified by comparing with MoM for a single rectangular scatterer. For simplicity, angular dependency of Keller's diffraction coefficient is replaced by Fresnel zone number (FZN). The method is applied in more real environment, for two rectangular plate of different dimensions in staggered arrangement. Next the staggered arrangement of two plates is changed to overlap each other when it is seen from source or some part of observation positions. The invisible integration points from source or the observer are excluded from the MER EEC line integration and the results without mutual coupling effect between plate or multiple diffraction between edges, shows excellent agreement with the reference solutions. From this study it is concluded that MER EEC gives very accurate result in less computation time. Replacement of angular dependency of Keller's diffraction coefficient by FZN does not degrade the accuracy but the method becomes more simpler. Shadowing effect for 10 GHz and 60 GHz for same scattere have been presented and it is computationally observed that shadowing is much more effective due to increase of frequency.

References

[1] M. Zhang, K. Tokosaki, J. Hirokawa, M. Ando, T. Taniguchi, and M. Noda, "A 60 GHz-Band Compact-Range Gigabit Wireless Access System using Large Array Antennas," *IEEE Transactions on Antennas and Propagation*, vol. 63, no. 8, pp. 3432–3439, Aug. 2015.

[2] Makoto Ando, "Antennas and propagation for millimeter wave compact range communication," in *International Symposium on Antenna and Propagation (ISAP) - 2014*, Kaohsiung, Taiwan, Dec. 2014, (Plenary Speech).

[3] J. B. Keller, "Geometrical Theory of diffraction," *J.Opt. Soc. Amer.*, vol. 52, pp. 116–130, Feb. 1962.

[4] R. G. Kouyoumjian and P. H. Pathak, "A uniform geometrical theory of diffraction for an edge in a perfectly conducting surface," *Proceedings of the IEEE*, vol. 62, no. 11, pp. 1448 – 1461, Nov. 1974.

[5] J. Boersma and P. H. M. Kerstan, "Uniform Asymptotic theory of electromagnetic diffraction by a plane screen," *(in Dutch) Tech. Rept.,Department of Math., Tech. University of Eindhoven, Eindhoven, the Netherlands*, 1967.

[6] D. S. Ahluwalia, R. M. Lewis, and J. Boersma, "Uniform asymptotic theory of diffraction by a plane screen," *SIAM J. Appl. Math*, vol. 16, pp. 783–807, 1968.

[7] S. W. Lee and G. A. Deschamps, "A uniform asymptotic theory of electromagnetic diffraction by a curved wedge," *IEEE Transactions on Antennas and Propagation*, vol. 24, no. 1, pp. 25–34, Jan. 1976.

[8] M. Ali, T. Kohama, and M. Ando, "Modified edge representation (MER) consisting of keller's diffraction coefficients with weighted fringe waves and its localization for evaluation of corner diffraction," *IEEE Transactions on Antennas and Propagation*, vol. 63, no. 7, pp. 3158–3167, Jul. 2015.

[9] M.Ali and M. Ando, "Fast estimation of shadowing effects in millimeter-wave short range communication by modified edge representation (MER)," *Communications, IEICE Transactions on*, vol. E98-B, no. 9, pp. 1873–1881, Sep. 2015.

[10] B. M. Kolundzija, J. S. Ognjanovic, and T. K. Sarkar, *WIPL-D: Electromagnetic Modeling of Composite Metallic and Dielectric Structures - Software and User's Manual*. Boston, London: Artech House, 2000.

[11] T. Murasaki and M. Ando, "Equivalent edge currents by the modified edge representation: Physical optics components," *Electronics, IEICE Transactions on*, vol. E75-c, no. 5, pp. 617–624, May 1992.

[12] T. Murasaki, M. Sato, Y. Inasawa, and M. Ando, "Equivalent edge currents for modified edge representation of flat plates: Fringe wave components," *Electronics, IEICE Transactions on*, vol. E76-c, no. 9, pp. 1412–1419, Sep. 1993.

[13] Constantine A. Balanis, *Advanced Engineering Electromagnetics*. New York: John Wiley & Sons Inc., 1989.